APPENDIX B. INTERIM PROGRESS REPORT, OCTOBER 1, 1978-DECEMBER 31, 1979 (FOR THE MASSACHUSETTS INSTITUTE OF TECHNOLOGY)

MASSACHUSETTS INST. OF TECH., CAMBRIDGE

1979

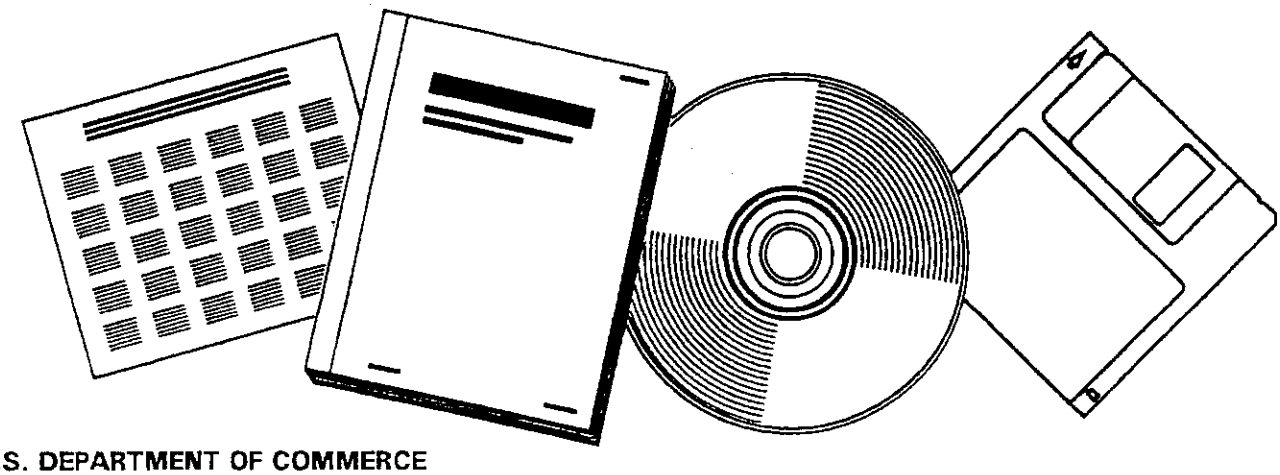

U.S. DEPARTMENT OF COMMERCE
National Technical Information Service

APPENDIX B

DOE/ET/13376--T1

DE84 009345

INTERIM PROGRESS REPORT FOR PERIOD OCTOBER 1, 1978 TO DECEMBER 31, 1979

by
Charles N. Satterfield, John P. Longwell
and George A. Huff, Jr.

DOE/ET/13376-T1

I. EXPERIMENTAL REACTOR SET-UP

The main experimental criterion has been to design a slurry-bed reaction unit which would yield kinetic information that could be analyzed by a straightforward, differential-rate approach and be free from experimental artifacts. With this in mind, a mechanically stirred autoclave reactor has been employed to provide a uniform gas, liquid and solid composition. Preliminary experimental runs of the unit have pointed out several flaws in our original design and the apparatus has been substantially re-constructed. Although more operator attention is now required, the apparatus is evolving into a reliable and precise piece of equipment. Throughout the design and construction of the experimental unit, safety has been an overriding concern. The apparatus can operate unattended for up to 24 hours since the synthesis gas feed and reactor furnace are automatically shut-down in the event that: (1) CO concentration in the laboratory air exceeds 50 ppm (OSHA limit); (2) reactor temperature, gas feed rate, or autoclave pressure substantially deviate from their set-point; (3) electrical power failure; or (4) ventilation of reactor off-gases fails.

Materials. The CO/H_2 mixed gas is custom blended from technical grade carbon monoxide and prepurified hydrogen by Matheson Gas Company. The gases are further purified with the use of adsorbents, filters, and dryers.

Normal-octacosane of 99%+ purity, synthesized by Humphrey Chemical Company, is employed as the slurry liquid as it is a high boiling (430°C at atmospheric pressure), relatively inexpensive, normal paraffin that is characteristic of waxes produced by the Fischer-Tropsch synthesis. Also, the product analysis is much simpler to perform with this pure slurry liquid.

The catalyst for our first shake-down studies is fused iron of composition 30-37 FeO: 58-65 Fe_2O_3: 2.0-3.0 Al_2O_3: 0.5-0.8 K_2O: 0.7-1.2 CaO, manufactured by United Catalysts and Chemicals, Inc. (United Catalysts, Inc.) under license agreement with Norsk Hydro of Norway and is designated as type C-73-1-01. While this catalyst is commercially employed for ammonia synthesis, it is quite similar to the composition used at the SASOL Fischer-Tropsch plant in South Africa.

Apparatus. The experimental unit is illustrated in Figure 2. It can be used at pressures up to 4 MPa and temperatures of 325°C, and is fabricated of stainless steel and Teflon. Operation is semi-batch in the sense that the synthesis gas (carbon monoxide

and hydrogen) is continually fed to the reactor and product vapors removed overhead while the liquid medium and catalyst are charged as a batch at the beginning of an experimental run.

Premixed hydrogen and carbon monoxide are first passed through 13X-molecular sieve and activated carbon traps for further purification and then through a 2-micron filter. The flow of gas is controlled by a Badger-Precision pneumatic metering valve, Rosemount differential-pressure cell, and Foxboro P.I.D. controller in a feedback control loop. The gas flow out of the reactor is measured either with a wet-test meter after saturation with water vapor or with a soap-film bubblemeter. The unit pressure is controlled by a dome-loaded back-pressure regulator at room temperature. As shown in Figure 2, the condensable products are recovered in two stages. Waxes and heavy products are collected in the first state that is operated at about 80°C and reactor pressure. The lighter products are trapped at atmospheric pressure in a knockout pot immersed in a water bath that is maintained at 2°C by mechanical refrigeration. Residual gases are separated and analyzed by gas chromatography with the implementation of an on-stream, Valco gas-sampling valve.

During initial experimental runs, plugs periodically developed in the stainless-steel tubing that connected the reactor with the wax trap and was heated to 300°C (to avoid premature product condensation) at reaction pressure. Upon examination of the tubing, the interior wall was found to be heavily coated with a carbonaceous residue. Most likely, the carbon was formed by the decomposition of carbon monoxide to carbon and carbon dioxide (Boudouard reaction) as this reaction reportedly proceeds at a significant rate with CO/H_2 mixtures over an iron catalyst at 300°C and elevated pressures. Apparently, the iron in the stainless-steel tubing substantially promotes this undesirable reaction. The problem has been substantially overcome by minimizing this hot tubing length and by using glass-lined, stainless-steel tubing to eliminate contact of the products with the stainless steel. In addition, Teflon-coated, stainless-steel tubing, maintained at 100°C, is utilized between the two condensate traps to further prevent any deleterious interaction of the reaction products with the experimental apparatus.

The synthesis is carried out in a one-liter, mechanically-stirred autoclave which is operated to behave as a CSTR in which the composition of its contents are uniform. The autoclave is heated by a two-zone, lapped furnace that fits snugly around the unit. The heat input on one zone is preset by a Genrad variac while the amount of heat is regulated on the other zone by a Cardsman (West) controller so as to maintain an isothermal reactor temperature. A type-J thermocouple, located in a well in the autoclave, records reaction temperature with the help of an Omega digital thermometer. A liquid sampling tube is positioned in the reactor vessel with a two-micron filter at the tube inlet to strain the entrained catalyst from the liquid medium. Samples of the slurry liquid are analyzed by gas chromatography.

Reduction. Since a temperature of 450°C, required for a rapid reduction of the iron catalyst, would quickly boil-off the liquid medium in the slurry-bed reactor, the catalyst is reduced in a separate unit that is shown in Figure 3. The reduction tube is constructed of type-316 stainless steel and measures 1.6-cm I.D. by 40-cm long. Porous frits in the tube prevent carry-over and loss of the catalyst. An aluminum jacket fits securely around the stainless-steel tube to promote heat transfer and minimize axial temperature gradients. The reduction unit is located in a Lindberg tubular furnace. Reduction is carried out with prepurified hydrogen that is first passed through 13-X molecular sieve and activated carbon filters. Flow is maintained by a Fischer-Porter flow tube assembly with a needle valve. Two 1.5 cm I.D. by 48-cm long glass tubes, packed with moisture-indicating, 8-mesh Drierite, are located downstream of the reduction unit. As water is a by-product in the reaction of iron oxide with hydrogen to produce iron, the extent of reduction is followed by watching the rate that the Drierties changes color down the tube upon the removal of moisture from the gaseous effluent (from blue to violet). With a hydrogen space velocity of 1000 V/V/Hr at 450°C and atmospheric pressure, reduction is generally complete in about three days. The reduced catalyst is cooled to roon temperature and then transferred, under an inert helium blanket, to the autoclave reactor.

Analytical Procedure. Exit gases from the reactor are separated and analyzed by a Carle refinery gas analyzer, Model RGA-156A. The instrument employs three automated valves for switching components into one of three chromatographic columns in order to optimize the separation. It operates isothermally at 50°C with a thermal conductivity detector and helium as the carrier gas (27 cm^3/min). The first column consists of EEA and Squalane to detect butane and pentane isomers. CO_2, C_2 and C_3 gaseous hydrocarbons are then separated with a Porapak Q column. Methane, hydrogen, and carbon monoxide are separated finally on a 13-X molecular sieve column. The Carle analyzer employs a patented method for a rapid and accurate measurement of hydrogen concentration. This is accomplished by passing the hydrogen and helium carrier gas mixture through a transfer tube at 600°C in which hydrogen diffuses across the tube wall into a nitrogen carrier gas stream while helium does not penetrate it.

The carbon number distribution of the condensed products is obtained with a Perkin-Elmer 900-B gas chromatograph that uses a flame ionization detector and dual 3.3-meter by 2-mm I.D. columns. The columns are packed with 10% SP-2100 on 80-100 mesh Supelcoport. The column temperature is programmed from 60° to 350°C at 6°C/min and held at 350°C. Helium, flowing at 30 cm^3/min, is employed as the carrier gas.

Water and light alcohols are obtained with the same Perkin-Elmer 900-B gas chromatograph that now utilizes a thermal conductivity detector and 3.3-meter by 2-mm I.D. column. The column is packed with 60-80 mesh Tenax. The column temperature is held at 30°C for four minutes and then programmed to 350°C at 8°C/min and held at 350°C. Helium, flowing at 25 cm^3/min, is used as the carrier gas. The procedure for analyzing the chromatograms has been checked extensively with standard calibrated mixtures.

II. EXPERIMENTAL RESULTS AND DISCUSSION

Kinetic Model

A slurry-bed reactor for the highly exothermic, Fischer-Tropsch synthesis offers several advantages over more "classical" reactor configurations. Most notably, it eliminates "hot spot" formation that plagues fixed-bed operation and catalyst agglomeration from heavy wax condensation that ails fluidized-bed reactors, and permits the use of much lower H_2/CO ratios in the feed gas. On the other hand, the overall rate may be hindered by the rate of transport of the reactants from the gas bubbles, through the liquid medium, to the surface of the solid catalyst. Our preliminary experimental results verify that this mass transfer limitation can indeed limit the maximum rate and, perhaps even more important, alter the product distribution.

As implied above, a number of transport steps must occur before the synthesis gas can be converted to hydrocarbon products on the catalyst surface. For gaseous hydrogen and carbon monoxide that are sparged into the liquid medium, these stages (based on film theory) are:

(1) Transport of the CO and H_2 from the bulk gas phase to the gas bubble-liquid interface.
(2) Transport from the gas-liquid interface to the bulk liquid.
(3) Transport from the bulk liquid to the catalyst surface.
(4) Diffusion of the reactants into the porous catalyst, which occurs simultaneously with adsorption of the synthesis gas onto the catalyst surface, and then reaction to yield products.
(5) Desorption and transport of paraffinic products from the catalyst to the bulk liquid and gas (for volatile products).

These steps are illustrated in a concentration profile of the Fischer-Tropsch synthesis shown in Figure 4.

A number of simplifying assumptions concerning these steps are well justified for the Fischer-Tropsch synthesis over an iron catalyst in a slurry-bed reactor, based on experimental work reported by previous investigators. As outlined in our ISCRE-6 paper (Appendix A), it can be concluded that the overall rate of reaction is predominantly limited by mass transfer of the reactants from the gas bubbles to bulk liquid and by intrinsic kinetics.

Although intensive research and development for the Fischer-Tropsch, slurry reactor was carried out by Rheinpreussen in Germany, U.K. Fuel Research Station, and U.S. Bureau of Mines from World War II until the early 1960's it was not until 1963 that Calderbank et al. realized that mass transfer could limit the rate of synthesis in this three-phase reaction system. Excluding the work by Calderbank and his coworkers Farley and Ray (1964), all of the other workers have either been mistakenly led to the conclusion that mass transfer

does not affect their results, or more often, mass transfer has been neglected altogether. In as many cases as possible, we have reanalyzed these previously published studies to determine the extent to which they were affected by mass transfer. The procedure for our reexamination is detailed in our paper in Appendix A. The results are summarized in Table 1. Surprisingly, we discovered that all of the studies were probably at least moderately limited by mass transfer.

Recently, Zaidi et al. (1979) have published experimental evidence that appears to refute the earlier claims by Calderbank and coworkers that mass transfer limits the rate of the Fischer-Tropsch synthesis in a slurry reactor. However, upon closer inspection of Zaidi's method of analyzing for mass transfer control, it appears that there is a serious misconception. Zaidi incorectly implies that a transition zone in which the reaction rate can be partially limited by both surface reaction and mass transfer does not exist. Furthermore, it appears that Zaidi's experiments were conducted in this very transition regime.

Based on these earlier studies, the effect of mass transfer on the Fischer-Tropsch synthesis in a slurry reactor cannot be dismissed, and must be reckoned with in order to optimize reactor design and catalyst utilization. Our experimental results also suggest that the efficient operation with low ratio H_2/CO feeds, an advantage of slurry reactor operation, may be a beneficial consequence of mass transfer limitations.

Before we can discuss our results for a fused-iron catalyst, it is necessary to revise the kinetic model developed in Appendix A for a bubble column reactor to our experimental apparatus in which the reactor contents are well-mixed. As noted in the ISCRE-6 paper, several workers have independently developed essentially the same kinetic rate model for the Fischer-Tropsch synthesis over an iron catalyst. For conversions up to at least 60%, the rate of disappearance of synthesis gas is first-order with respect to hydrogen concentration and zero order with respect to carbon monoxide. This implies, as substantiated by non-reacting adsorption studies, that carbon monoxide is much more strongly adsorbed on the catalyst surface than hydrogen and other reaction products, and so essentially saturates it. Also, since the rate is based on the disappearance of hydrogen plus carbon monoxide, it is conveniently independent of the water-gas-shift reaction, which occurs simultaneously with the Fischer-Tropsch reaction. It is assumed that the Boudouard reaction proceeds minimally in comparison to the Fischer-Tropsch reaction at temperatures less than about 300°C.

From a thermodynamic viewpoint, the rate of reaction in the absence of intraparticle diffusion should be the same for the liquid and vapor phases, if it is assumed that the liquid does not participate in the reaction. When the intrinsic rates for vapor-phase operation, based on reactant partial pressure, and liquid-phase reaction, based on liquid concentration, are expressed as the same chemical potential driving force, they are related by:

$$k_{vp}/k_{sb} = 1/RTm_H \qquad (1)$$

Therefore, the rate of reaction for the Fischer-Tropsch synthesis over an iron catalyst per unit volume of slurry can be expressed as:

$$R_{CO+H_2} = R_{CO} + R_{H_2} = -k_{sb}(1-\varepsilon_G)wC_{H,L} \qquad (2)$$

(Note that we intend to investigate the applicability of this intrinsic rate expression during the course of our work.)

The material balance of hydrogen over the differential, well-stirred reactor is given by:

$$Q\left[C_{H,G_i} - C_{H,G_o}\right] = V_L k_{L,H}a\ (C^*_{H,L} - C_{H,L}) \qquad (3)$$

where it is assumed that the major physical resistance is transfer of hydrogen across the gas-liquid interface to the bulk liquid, and that equilibrium is established at the gas-liquid interface, i.e. $C^*_{H,L} = C_{H,G_o}/m_H$. Hence the rate of gas absorbed per unit volume of slurry is:

$$R_{H_2} = \frac{Q\left[C_{H,G_i} - C_{H,G_o}\right]}{V_L} = k_{L,H}a\left[\frac{C_{H,G_o}}{m_H} - C_{H,L}\right] \qquad (4)$$

At steady-state, the rate of gas absorbed is equivalent to the rate of reaction. Solving Equation 2 for $C_{H,L}$ and substition into Equation 4 results in the following, upon simplification:

$$\frac{QX_{H_2}m_H(1-\varepsilon_G)}{k_{L,H}aV_L^\circ} + \frac{GX_{H_2+CO}\ (1+S)}{S\ V_L^\circ\ k_{vp}P\omega} = 1 - X_{H_2} \qquad (5)$$

where the pseudo-intrinsic, vapor-phase rate constant, k_{vp}, has been defined by Equation 1. By this mathematical manipulation, we can directly compare activation energies obtained for k_{vp} from our liquid-phase studies to values reported by others in vapor-phase operation. It should be emphasized that this approach is completely rigorous so long as the liquid is "inert" and does not appreciably adsorb on the catalyst surface, which we believe to be the case as paraffins are the least strongly absorbed hydrocarbons.

For simplicity, an overall rate constant can be calculated from properties that are obtained directly from our experimental apparatus, i.e., temperature, catalyst weight, pressure, conversion, inlet flow rate, and hydrogen to carbon monoxide inlet feed ratio. This expression is given by:

(6)

$$k^* = \frac{(S+1)}{S}\ \frac{GX_{H_2+CO}}{PV_L^\circ\omega\left[1-X_{H_2}\right]}$$

From Equation 5, it can be easily shown that the overall rate constant, k°, is really a combination of intrinsic and mass transfer components.

$$\frac{1}{k^\circ} = \frac{1}{k_{vp}} + \frac{RT\, m_H (1-\xi_G)\omega\, X_{H_2}}{k_{L,H}\, a\, X_{H_2+CO}}\left(\frac{S}{1+S}\right) \qquad (7)$$

overall intrinsic mass transfer

From this expression, we can make some comments about it based on previous work on the Fischer-Tropsch synthesis in the vapor phase for an iron catalyst, and founded on our experience with mass transfer in general. First the intrinsic component reportedly has an activation energy of 17 to 27 kcal/mole (Appendix A) while the mass transfer term should be around 5 kcal/mole. In other words, there is a striking difference for the temperature dependency of mass transfer and intrinsic reaction that make up the overall rate constant. As is often the case, intrinsic kinetics dominate at lower temperatures but mass transfer at higher temperatures. Second, when only the degree of agitation is changed, the mass transfer term will vary while the intrinsic rate component remains constant. Specifically, for our experimental apparatus, gas bubble size decreases and gas hold-up increases as the shear-rate increases with more rapid stirring speeds. As a result, there is more gas in the slurry with a larger surface area for mass transport, and, hence, the mass transfer component diminishes as agitation increases. For this report, we shall dwell on the rate of synthesis gas disappearance. However, preliminary evidence will be presented to suggest that mass transfer also markedly affects the product distribution.

Experimental Results

72.8 grams of fused-iron catalyst, manufactured by United Catalyst, Inc., was ground to 80 to 100 mesh size. Upon reduction with hydrogen at 440°C with a space velocity of 1000 v/v/hr for about 72 hours, it lost 18.3 grams of oxygen as water. The material, under a helium blanket, was charged into the reactor which was filled with inexpensive paraffin wax, sold by Fisher Scientific as P-21 Paraffin, that melts at 53-57°C. The reactor was pressurized to 100 psig (690 kPa), and the synthesis gas ($H_2/CO = 1.58$) flow was set at 955 cm^3 at S.T.P./min. which corresponds to a liquid hourly space velocity of 115 cm^3 gas at S.T.P./cm^3 liquid/hr. With 400 grams of paraffin charged to the reactor with a density of about 0.8 g/cm^3, the catalyst loading was 109 grams of reduced catalyst/liter slurry. The stirrer speed was set at 750 RPM, and the reactor was quickly heated to reaction conditions. Steady-state operation was rapidly achieved with the iron catalyst and there was no noticeable decline in catalytic activity over the duration of the investigation, which lasted for a week. Experimental conditions were changed after three samples indicated that a constant state had been achieved.

In Figure 5 the overall rate constants, calculated from Equation 6, are plotted against reciprocal temperature as in the Arrhenius form. The raw experimental data are summarized

in Table II. For this figure, only temperature, and consequently conversion, were changed. For temperatures lower than about 260°C, a linear fit is obtained with an activation energy of about 17.5 kcal/mole. However, at temperatures greater than 260°C, the activation energy begins to decline. This is almost a textbook example of the appearance of mass transfer limitations. Furthermore, the value of 17.5 kcal/mole is in excellent agreement for the intrinsic activation energy of 17 to 27 kcal/mole reported for an iron catalyst in a vapor-phase, fixed-bed reactor.

We further investigated the reaction by holding the temperature at 260°C and varying only the rate of agitation by changing stirrer speed. All other conditions were identical to those employed for the preceding runs. Not surprisingly, it is observed (Figure 6) that the overall rate constant increases to an asymptotic value at a high degree of agitation, i.e. greater than about 750 RPM. In other words, mass transfer becomes increasingly dominating at lower stirring speeds as the rate of mass transfer is artificially slowed. These results agree nicely with those reported in Figure 5, as both figures indicate that slight mass transfer limitations exist at 750 RPM and 260°C for our particular set of conditions.

The ratio of olefin to paraffin for C_6, C_{11}, and C_{13} hydrocarbons for the same runs illustrated in Figure 6 is plotted against stirring speed in Figure 1. The olefin to paraffin ratio decreases as mass transfer becomes more controlling, i.e. lower stirring speed. This result is easily explained when it is remembered that hydrogen has a greater diffusion rate in the liquid medium, and hence, a larger mass transfer coefficient than carbon monoxide. As a consequence, the catalyst surface becomes lean in CO and rich in hydrogen as mass transfer sets in. Since it has been well documented that the ratio of olefin to paraffin decreases as the H_2/CO ratio increases for vapor-phase, fixed-bed operation, it is not surprising then that the ratio of olefin to paraffin decreases as mass transfer becomes increasingly important in a slurry-bed reactor. This observation explains basically at least one of the reasons for a claim that is often made in the literature, that slurry reactors can accomodate a lower H_2/CO feed without drastically affecting catalyst performance and product selectivity, which would normally occur in vapor-phase operation.

Reactor Modifications

The experimental unit has undergone recent extensive modification to permit an accurate determination of reaction products. In particular, we had employed on-line, gas sampling valves heated at 300°C to avoid product condensation, but discovered that leaks periodically developed as they could not continually withstand this harsh temperature. One such leak prematurely ended the experimental runs reported above and caused a thermal conductivity detector in a gas chromatograph to fail after subjecting it to air at its operating temperature of 350°C. Upon reevaluation of the situation, it was decided to condense and collect product samples, as indicated in Section I, and subsequently inject them into the gas chromatograph by syringe. Only noncondensable gases, i.e., methane through butane, CO, H_2, and CO_2, are still sampled at

50°C with an on-line, gas sample valve. We expect to commence data acquisition again very shortly.

III. Nomenclature

a	interfacial area of gas bubbles, cm^2 gas bubble area/cm^3 expanded liquid
$C_{H,G}$	concentration of hydrogen in gas phase, mol/cm^3 gas; C_{H,G_i} for reactor inlet; C_{H,G_o} for reactor outlet; $C_{H,L}$ for liquid phase, mol/cm^3 liq., $C^*_{H,L}$ for concentration in liquid at equilibrium with the gas.
E_a	activation energy, kcal/mol
G	molar flow of synthesis gas, mol gas/sec
$k_{L,H}$	liquid film mass transfer coefficient for hydrogen, cm^3 liq./(cm^2 gas-bubble surface area)(sec)
k°	overall reaction rate constant in the liquid-phase, mol/(g cat.)(MPa); k_{sb} for intrinsic reaction rate constant in a slurry-bed reactor, cm^3 liq./(g cat.)(sec); k_{VP} for intrinsic reaction rate constant in a vapor-phase, fixed-bed reactor, mol/(g cat.)(sec)(MPa).
m_H	solubility coefficient of hydrogen in liquid, cm^3 liq./cm^3 gas
P	total reaction pressure, MPa
Q	volumetric flow of synthesis gas, cm^3 gas/sec
R	ideal gas constant, 8.2 (MPa)(cm^3 gas)/(mol)(°K)
R_i	rate of gas i absorbed per volume of slurry, mol/(cm^3 expanded liq.)(sec)
S	ratio of hydrogen to carbon monoxide in the feed gas, mol H_2/mol CO
T	absolute reaction temperature, °K
V_L	volume of expanded slurry, cm^3 expanded liq.; V°_L for volume of unexpanded liquid, cm^3 liq.
X_i	conversion of gas i, e.g. $X_{H_2} = \left[C_{H,G_i} - C_{H,G_o}\right]/C_{H,G_i}$

Greek

ϵ_G	fractional gas hold-up
ω	catalyst loading, g cat./cm^3 liq.

References to Appendix B

Calderbank, P., F. Evans, R. Farley, G. Jepson, and A. Poll (1963). "Catalysis in Practice", Symp. Proceed. (Instn. Chem. Engrs.), 66.

Farley, R. and D. Ray (1964). J. Inst. Petr., 50, 27.

Hall, C., D. Gall, and S. Smith (1952). J. Inst. Petr., 38, 845.

Kölbel, H. (1947). In BIOS Final Report No. 1712, 7 pp.

Kölbel, H. and P. Ackermann (1949). U.S. Bur. Mines Translation K-10.

Kölbel, H. and P. Ackermann (1951). Proceed. Third World Petr. Congress, Section IV, 2.

Kölbel, H., P. Ackermann, and F. Engelhardt (1955). Proceed. Fourth World Petr. Congress, Section IV, 227.

Kölbel, H. and P. Ackermann (1956). Chemie-Ing.-Technik, 28(6), 381.

Mitra, A. and A. Roy (1963). Indian Chemical Engineer, 127.

Sakai, T. and T. Kunugi (1974). Sekiyu Gakkai Shi, 17 (10), 863.

Schlesinger, M., H. Benson, E. Murphy, and H. Storch (1954). Ind. Eng. Chem., 46, 1322.

Schlesinger, M., J. Crowell, M. Leva, and H. Storch (1951). Ind. Eng. Chem., 43, 1474.

Zaidi, A., Y. Louisi, M. Ralek, and W. Deckwer (1979). Ger. Chem. Eng., 2, 94.

TABLE 1. FISCHER-TROPSCH, SLURRY REACTOR RESEARCH

Investigator	Temperature (°C)	Pressure (atm)	Mass Transfer Limitations
Farley and Ray (1964) Fuel Research Station, UK	200 - 285	1.5 - 11	Severe Above 260°C
Calderbank et al. (1963) Fuel Research Station, UK	265	11 - 22	Severe
Hall, Gall and Smith (1952) Fuel Research Station, UK	260 - 320	21 - 41	?
Sakai and Kunugi (1974) Nagoya City University, Japan	200 - 290	11 - 14	Severe
Schlesinger et al. (1951 & 1954) USBM, US	220 - 280	8 - 21	Severe Above 245°C
Mitra and Roy (1963) Indian Inst. of Tech., India	240 - 265	8 - 11	?
Kolbel et al. (1947, 1949, 1951, 1955, 1956) Rheinpreussen, Germany	200 - 320	8 - 30	?
Zaidi, A., Y. Louisi, M. Ralek, W. Deckwer, Germany (1979)	250 - 290	9	Moderate

TABLE II. EXPERIMENTAL RESULTS FOR THE FISCHER-TROPSCH SYNTHESIS OVER AN IRON CATALYST IN A SLURRY-BED REACTOR.

750 RPM, 1.58 H_2/CO, 100 psig

Reactor Temperature

	25°C	204°C	218°C	236°C	260°C	266°C	275°C	293°C
Flow rate of Noncondensable Gases, ℓ/min	.955	.832	.785	.711	.584	.517	.499	.454
X_{H_2}, %	--	14.6	20.8	28.6	44.4	49.7	52.1	57.6
X_{CO}, %	--	14.0	23.1	37.1	73.6	83.3	89.3	94.0
X_{CO+H_2}, %	--	13.6	21.7	31.9	55.7	62.7	66.5	71.7

260°C, 100 psig, 1.58 H_2/CO

Stirring Speed

	250 RPM	500 RPM	750 RPM	1000 RPM	1250 RPM
Flow rate of Noncondensable Gases, ℓ/min	.800	.675	.584	.557	.557
X_{H_2}, %	19.2	31.8	44.4	44.4	44.4
X_{CO}, %	18.2	50.6	73.6	77.9	77.9
X_{CO+H_2}, %	18.9	39.1	55.7	57.4	57.4

FIGURE 1. EFFECT OF AGITATION ON PRODUCT SELECTIVITY OF THE FISCHER-TROPSCH SYNTHESIS IN A SLURRY-BED REACTOR

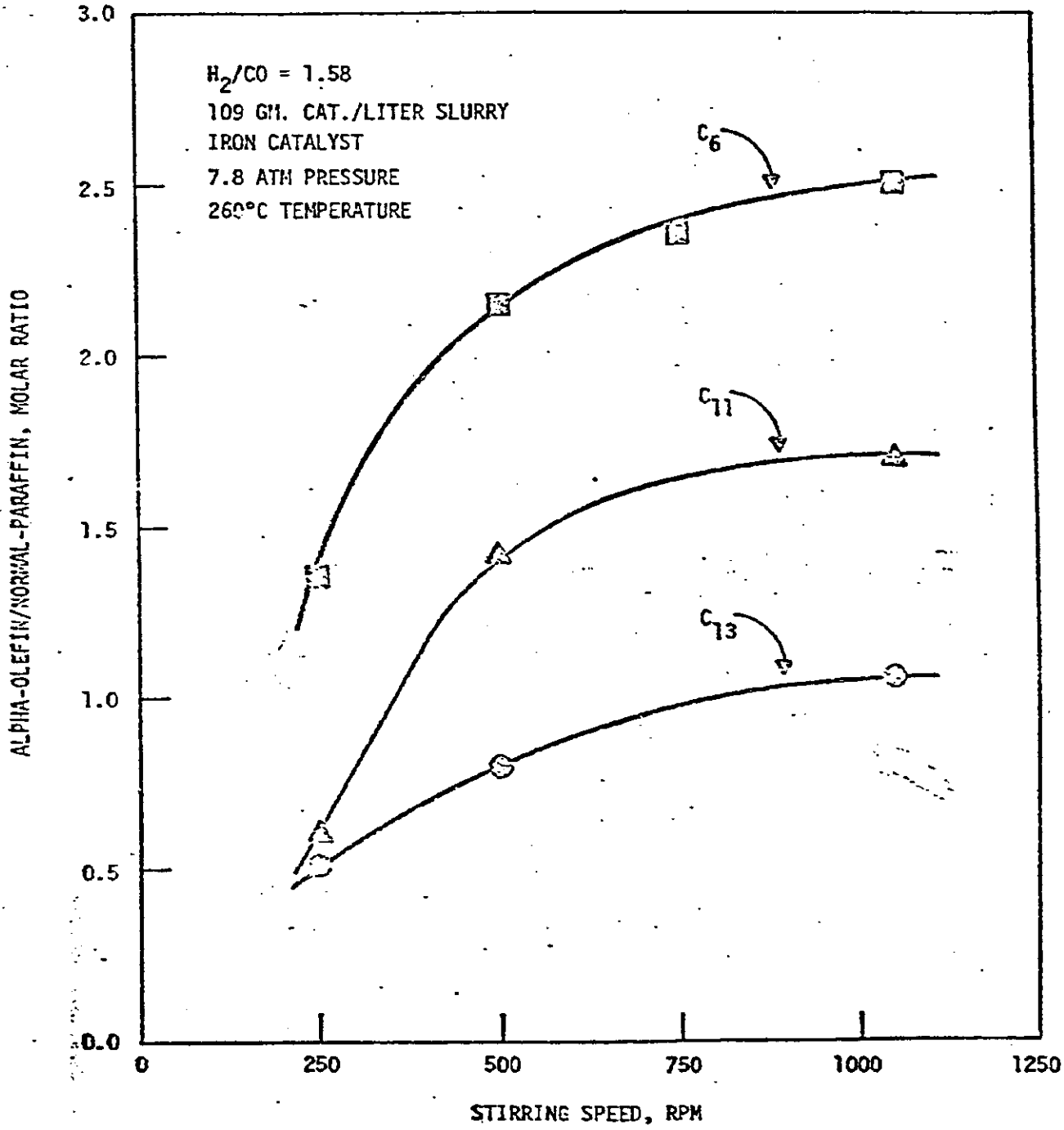

A Pressure Regulator
B Filter Dryer
C Differential-Pressure Cell
D Pneumatic Control Valve
E Needle Control Valve
F Back-Pressure Regulator
G Condensed Products
H Electric Furnace
I Thermocouple
J Baffle
K Magnedrive Stirrer
L Pressure Gauge
M Knockout Pot
N Gas Sample Valve
O Soap-Film Flowmeter
P Water Saturator
Q Wet-Test Meter
R Slurry Sample Tube
S Turbine Impeller

FIGURE 2. FISCHER-TROPSCH, SLURRY-BED REACTION UNIT

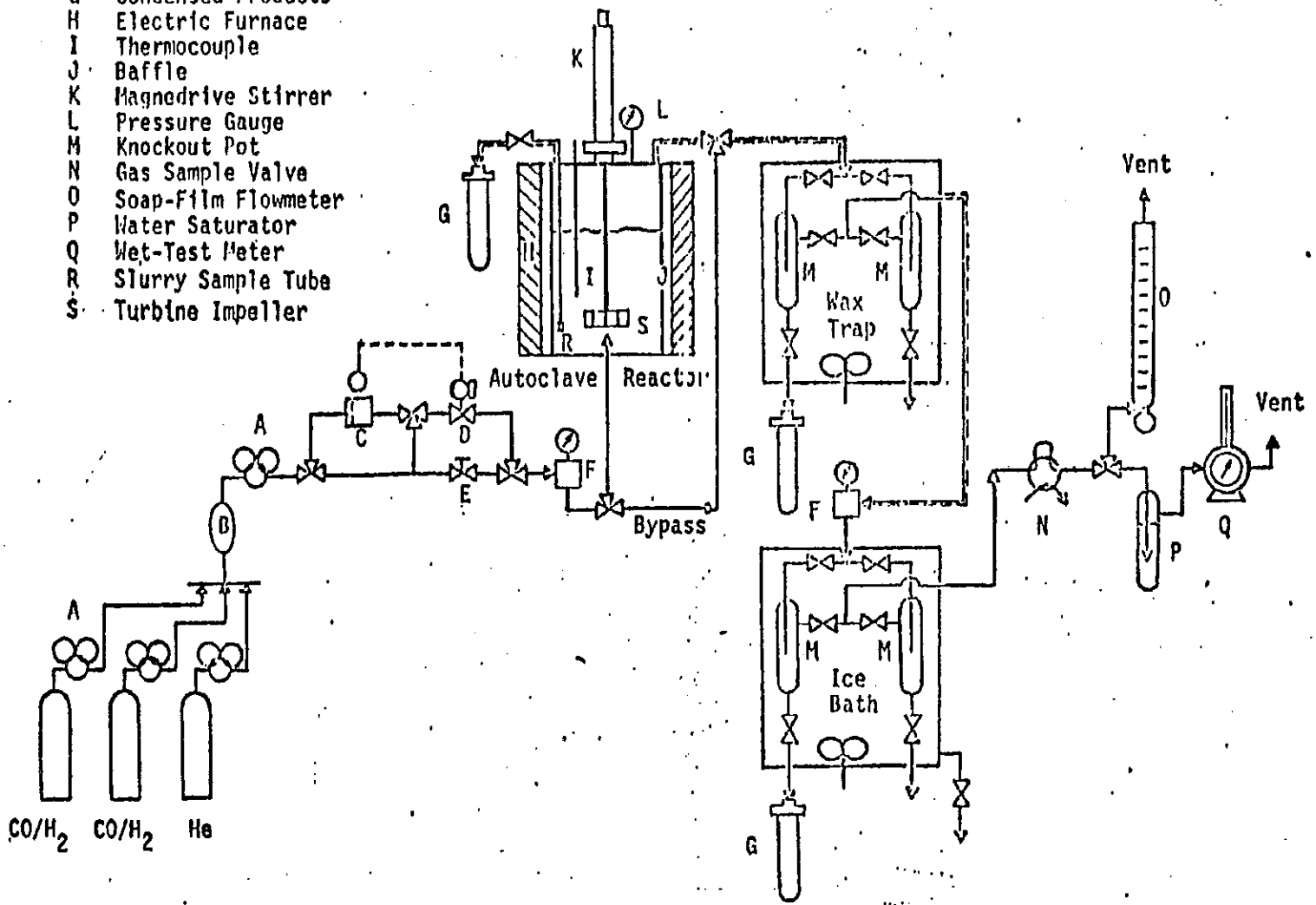

A Pressure Regulator
B Filter Dryer
C Needle Control Valve
D Rotameter
E 2-Micron Porous Frit
F Aluminum Jacket
G Electric Tube Furnace
H Thermocouple
I Columns Packed with Drierite
J Water Saturator
K Wet-Test Meter

FIGURE 3. REDUCTION UNIT FOR FISCHER-TROPSCH CATALYSTS

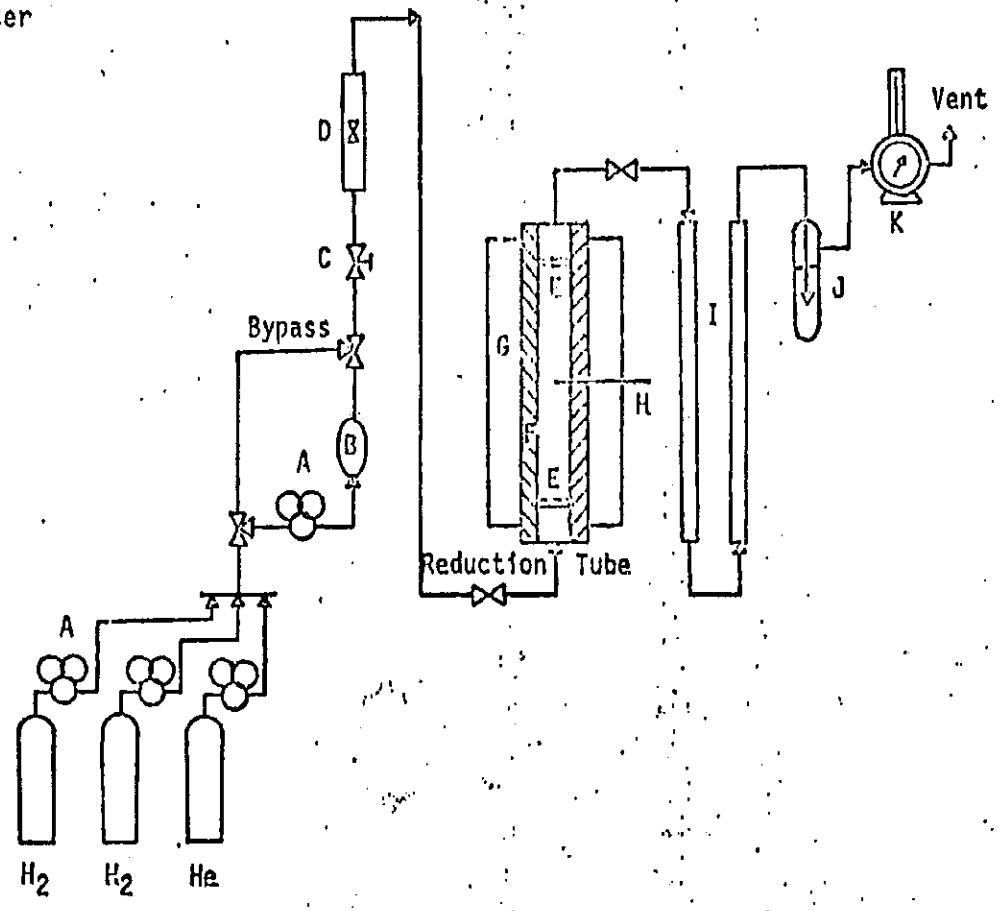

FIGURE 4. CONCENTRATION PROFILE OF THE FISCHER-TROPSCH SYNTHESIS IN A SLURRY-BED REACTOR

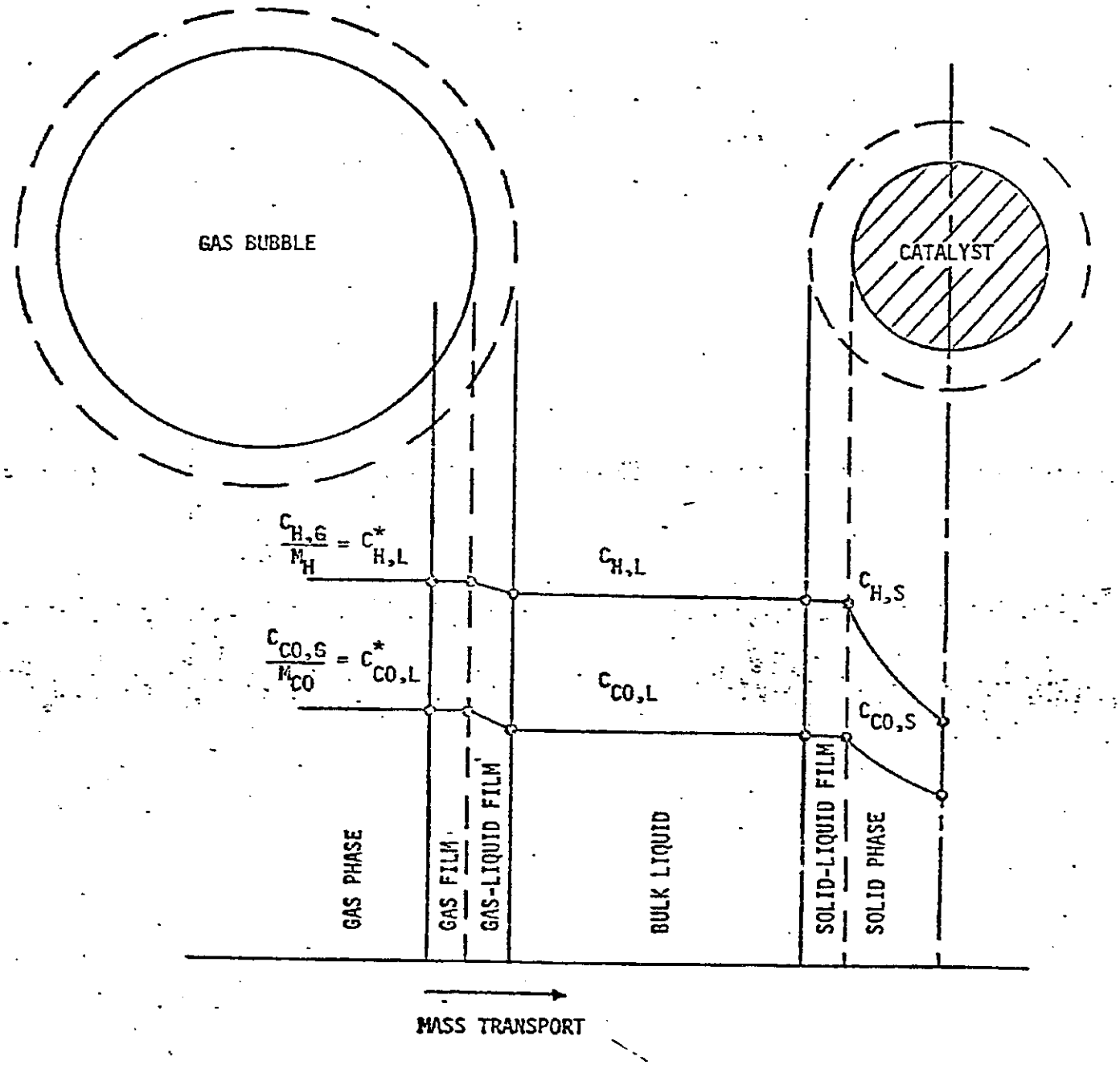

FIGURE 5. EFFECT OF TEMPERATURE ON THE FISCHER-TROPSCH SYNTHESIS IN A SLURRY-BED REACTOR

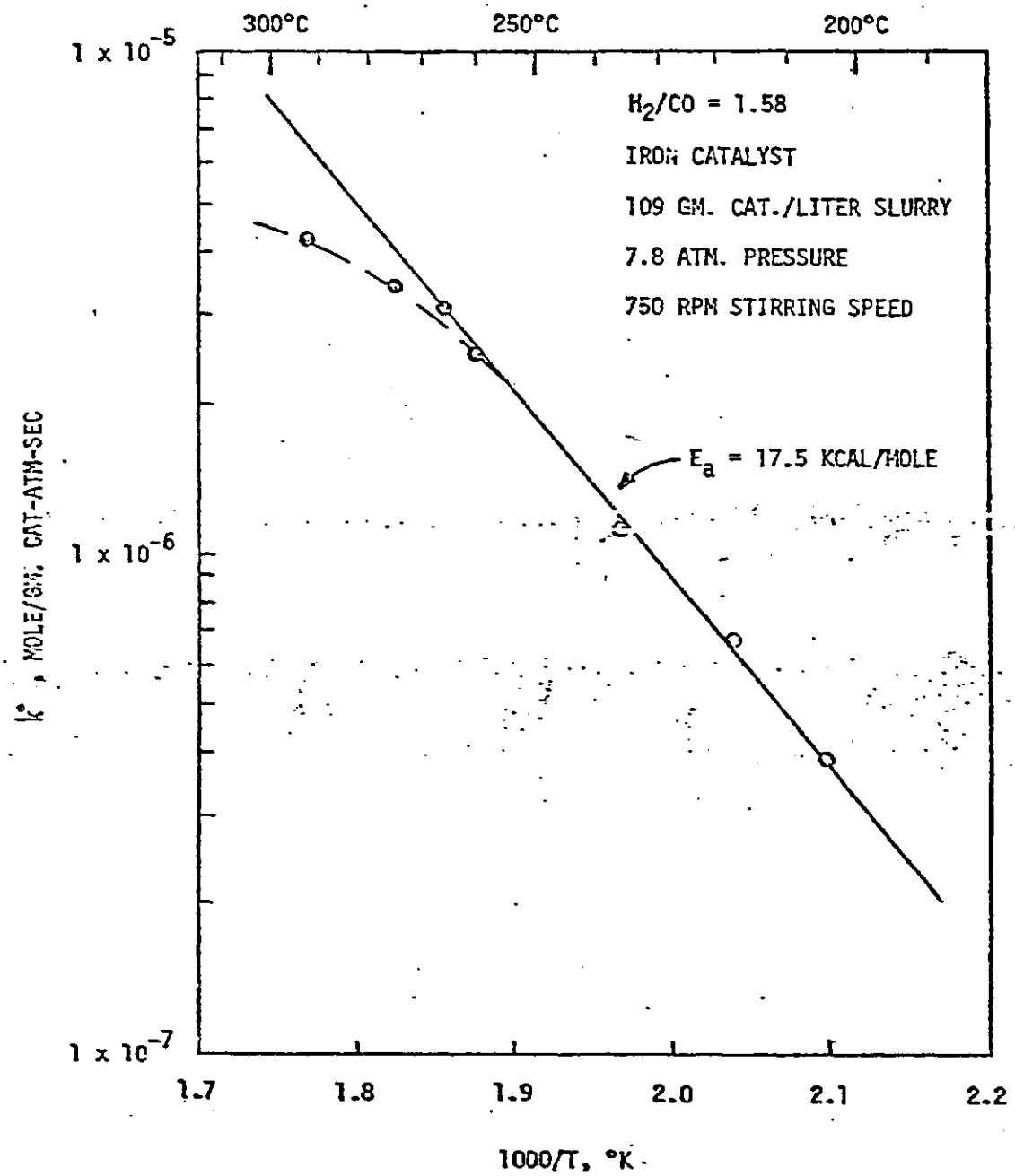

FIGURE 6. EFFECT OF STIRRING SPEED ON THE FISCHER-TROPSCH SYNTHESIS IN A SLURRY-BED REACTOR

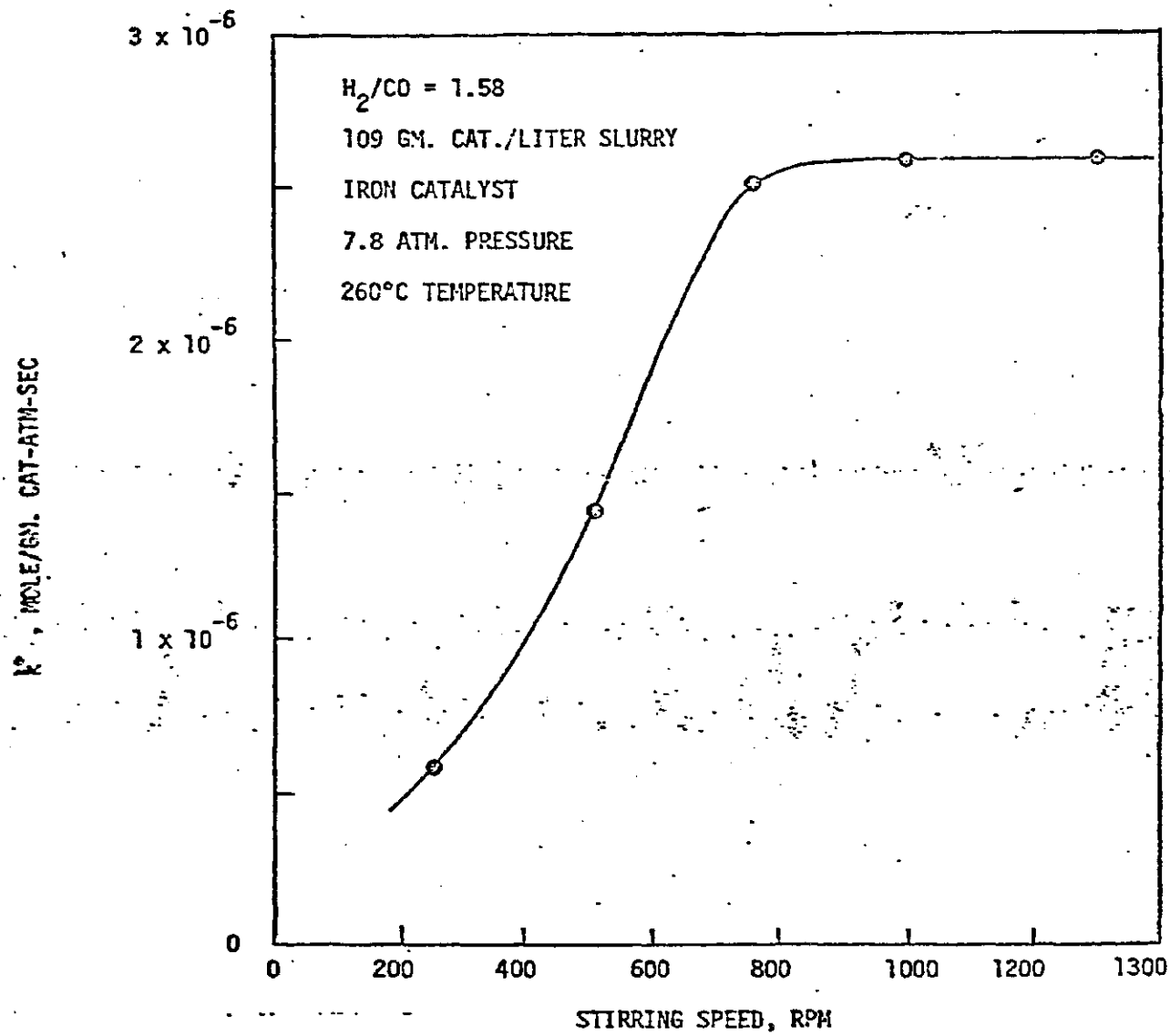

DISCLAIMER